Available online at www.sciencedirect.com
SCIENCE DIRECT®
Biochimica et Biophysica Acta 1616 (2003) 95–105
BIOCHIMICA ET BIOPHYSICA ACTA
BBA
www.bba-direct.com

# Selective amphipathic nature of chlorpromazine binding to plasma membrane bilayers☆

James Y. Chen[a,b,1], Linda S. Brunauer[b], Felicia C. Chu[a], Colleen M. Helsel[b], Margaret M. Gedde[a,2], Wray H. Huestis[a,*]

[a] *Department of Chemistry, Stanford University, 380 Roth Way, Stanford, CA 94305-5080, USA*
[b] *Department of Chemistry, Santa Clara University, Santa Clara, CA 95053, USA*

Received 4 February 2003; received in revised form 6 June 2003; accepted 17 July 2003

**Abstract**

Chlorpromazine (CPZ), an antipsychotic agent shown to inhibit the action of various neurophysiological receptors, also exhibits preferential association with the plasma membrane, inducing stomatocytic morphological response in red blood cells (RBC). Given the cationic nature of CPZ, fluorimetry, pH titration, and red cell morphological studies were performed to assess the associative predilection of CPZ for anionic membrane components. CPZ fluorescence intensity increased 320–370% upon addition of phosphatidylcholine (PC) small unilamellar vesicles (SUVs) to aqueous CPZ, indicating an affinity of the drug for lipidic phases. After removal of unbound drug, CPZ fluorescence increased up to 92% with increasing phosphatidylserine (PS) in the lipid phase (up to 30 mol% of total lipid), suggesting a preferential association of the drug with anionic lipids. In studies of pH titration, the p$K_a$ of CPZ in the presence of Triton X-100 micelles or phospholipid SUVs increased with increasing anionicity of the lipidic phase [7.8 with Triton X-100, 8.0 with PC, 8.3 with phosphatidylglycerol (PG)], lending further support to preferential drug interaction with anionic lipidic components. At 0 °C, CPZ-induced red cell shape change was less extensive in cells made echinocytic by adenosine triphosphate (ATP) depletion, compared to cells made echinocytic by PS treatment following vanadate preincubation. This suggests that polyphosphoinositide lipids are CPZ membrane binding sites. Since polyphosphoinositide lipids are implicated as important intermediates in a number of receptor-mediated cell signaling pathways, evidence of association with these specific lipids provides a means by which psychoactive drugs may induce neurophysiological effects through direct interaction with general membrane components.


*Keywords:* Chlorpromazine; Electrostatic; Amphipathic; Membrane; Erythrocyte; Fluorescence

*Abbreviations:* ATP, adenosine triphosphate; CPZ, chlorpromazine; DAG, diacylglycerol; DLPC, dilauroylphosphatidylcholine; DLPS, dilauroylphosphatidylserine; DMPC, dimyristoylphosphatidylcholine; DMPG, dimyristoylphosphatidylglycerol; DMPS, dimyristoylphosphatidylserine; HCT, hematocrit; NADH, β-nicotinamide adenine dinucleotide; PA, phosphatidic acid; PBS, phosphate-buffered saline; PC, phosphatidylcholine; PG, phosphatidylglycerol; PI, phosphatidylinositol; $PIP_2$, phosphatidylinositol-4,5-bisphosphate; PS, phosphatidylserine; RBC, red blood cells; SUVs, small unilamellar vesicles; Tris, tris(hydroxymethyl)aminomethane

☆ Supported by National Institutes of Health Grant HL23787; an IBM Faculty Research Grant from Santa Clara University; an Undergraduate Research Grant from the Howard Hughes Medical Institute, awarded to F.C.C.; and National Science Foundation Grant CHE-9820382 (R.E.U.). A summer stipend for C.M.H. through the NSF-REU program is gratefully acknowledged.

* Corresponding author. Tel.: +1-650-723-2503; fax: +1-650-723-4817.
*E-mail address:* whh@stanford.edu (W.H. Huestis).
[1] Present address: SEED Intellectual Property Law Group PLLC, 701 Fifth Avenue, Suite 6300, Seattle, WA 98104.
[2] Present address: Pharmaceutical Development Consultants LLC, 1115 Rainbow Boulevard, #120, Salida, CO 81201.

0005-2736/$ - see front matter © 2003 Elsevier B.V. All rights reserved.
doi:10.1016/S0005-2736(03)00229-3

## 1. Introduction

The phenothiazine family of drugs has been shown to elicit a variety of neuroleptic effects. Chlorpromazine (CPZ), one of the better-known phenothiazines, is an antipsychotic agent used historically in the treatment of schizophrenia. CPZ is believed to exert its antipsychotic effects by blocking dopamine receptors; however, CPZ also exerts effects upon muscarinic and $\alpha_1$-adrenergic receptors, a possible reason for the many side effects associated with this treatment (reviewed in Refs. [1,2]; see also Refs. [3–6]). Recently, CPZ has been shown to hold promise as a treatment for prion-based afflictions [7].

Other than by the blockage of specific cellular receptors, the diverse effects of CPZ may also be attributable to the amphipathic nature of the drug. The tricyclic ring structure of CPZ is hydrophobic, partitioning with relative ease into the bulk hydrocarbon phase of membrane bilayer systems, while the tertiary propylamine tail region of the drug is hydrophilic, interacting well with the polar headgroup regions of membrane bilayers [8]. Moreover, at physiological pH, the propylamine chain of the drug is cationic. Because the inner leaflet of the human red blood cell (RBC) plasma membrane bilayer contains virtually all of the net anionic phospholipids [9,10], electrostatic attractive forces may sequester CPZ in the inner membrane leaflet [11]. In theory, such accessibility of CPZ to the cytofacial surface of the cell membrane would allow the drug to exert pharmacological effects via direct interaction with intracellular processes such as signal transduction or intracellular trafficking. In normal discoid RBC, preferential accumulation of CPZ expands the inner leaflet, causing the membrane to buckle inward to produce a stomatocytic morphology [11].

While many reports have discussed the importance of hydrophobic and electrostatic forces in the interaction of CPZ with membrane bilayers, detailed characterization of these forces and their role in drug–membrane associations is lacking. The relative extent to which CPZ–membrane interactions are dictated by hydrophobic versus electrostatic effects remains largely unclear. Further, it is unclear whether the electrostatic interactions of CPZ with the membrane are dictated more by the presence of the abundant anionic lipid phosphatidylserine (PS) (net charge $-1$ at physiological pH) or the polyphosphoinositide lipids (present in very small quantities in the membrane, but each carrying a localized net charge of $-3$ or $-5$ at physiological pH).

In this investigation, fluorescence and titration studies are presented elucidating the electrostatic nature of CPZ binding to membranes. In addition, preferential binding of CPZ to specific anionic phospholipid classes is examined through studies altering RBC membrane phospholipid content and transbilayer distribution.

## 2. Experimental procedures

### 2.1. Materials

Chlorpromazine hydrochloride (CPZ), sodium orthovanadate (vanadate), 25% glutaraldehyde solution (grade I), Triton X-100, dilauroylphosphatidylcholine (DLPC), dimyristoylphosphatidylcholine (DMPC), inosine, and adenosine were obtained from Sigma Chemical Co. (St. Louis, MO). Adenosine triphosphate (ATP) assay kit was obtained from Sigma Diagnostics (St. Louis, MO). Dimyristoylphosphatidylserine (DMPS) was obtained from Avanti Polar Lipids, Inc. (Alabaster, AL). Dilauroylphosphatidylserine (DLPS) was obtained from Calbiochem (San Diego, CA). Dimyristoylphosphatidylglycerol (DMPG) was obtained both from Sigma and Avanti. Penicillin–Streptomycin (lyophilized powder) was obtained both from Sigma and Gibco BRL (Gaithersburg, MD). All other chemicals were reagent grade.

### 2.2. Vesicle preparation

Stock lipid solutions (typically in chloroform ± methanol) were dried down under a gentle stream of argon or nitrogen, then resuspended in phosphate-buffered saline (PBS; 138 mM NaCl, 5 mM KCl, 7.5 mM sodium phosphate, 1 mM $MgSO_4$, 5 mM glucose, pH 7.4) or NaCl/tris(hydroxymethyl)aminomethane (Tris) buffer (140 mM NaCl, 10 mM Tris, pH 7.4). Suspensions were bath-sonicated to clarity, to produce small unilamellar vesicles (SUVs). In experiments employing PS, magnesium (and occasionally glucose) was omitted from PBS and sonication was carried out under argon. SUVs in CPZ titrations were prepared by probe sonication (Heat Systems, Inc., Farmingdale, NY), followed by brief centrifugation to pellet and remove metal debris.

### 2.3. Separation of free CPZ from CPZ bound to model membranes

Samples of SUVs (0.2–1 mM phospholipid, composed of DLPC plus 0–30 mol% DMPS) were incubated with up to 120 μM CPZ for at least 20 min at ambient temperature, incubation conditions allowing CPZ to induce stable stomatocytosis in RBC [12]. Samples then were subjected to ultrafiltration via centrifugation at $6000 \times g$, using Nanosep Omega ultrafiltration units having a molecular weight cutoff of 30 kDa (Pall Corporation, Ann Arbor, MI). This process allows low molecular weight components (such as free unbound drug molecules) to filter through (the filtrate), while retaining high molecular weight components (such as drug molecules associated with SUVs) atop the filter (the retentate). After washing ultrafiltration units twice with buffer by centrifugation, sample filtrates and retentates were resuspended in buffer (to 1 ml total volume each) and kept at 25 °C

for subsequent drug analysis by fluorimetry. Before sample application, ultrafiltration units were seasoned via centrifugation with CPZ (0.6–1.2 mM in 150 mM $NaCl_{(aq)}$), followed by extensive washing with 150 mM $NaCl_{(aq)}$ and NaCl/Tris buffer.

### 2.4. Fluorescence studies of CPZ in model membrane systems (after Ref. [13])

Filtrate and retentate solutions proceeding from ultrafiltration of CPZ-treated SUV samples were exposed to near-UV radiation and analyzed for emission signal intensity of CPZ fluorescence at the excitation and emission wavelengths indicated, for 3.5 min at 15-s intervals (Fluorolog-3 spectrofluorimeter, Model FL3-22, Instruments S.A., Inc., Edison, NJ). Drug fluorescence emission for each sample was expressed as the average of the final 105 s of readings. Alternatively, samples not subjected to ultrafiltration were analyzed for CPZ fluorescence emission signal intensity at the excitation and emission wavelengths indicated, by acquisition of single instantaneous signal readings.

### 2.5. Titration of CPZ in model membrane systems

CPZ (3.25 mM) and model membranes [micelles of 3.1% Triton X-100 (v/v)], or SUVs (22.5 mM DLPC with either 2.5 mM DMPC, DMPS, or DMPG) were combined, and suspended to an initial volume of 5 ml in 150 mM NaCl. Solutions then were acidified slightly past the neighboring equivalence point with HCl, before titrating with 0.25–0.5 M NaOH in 3-μl aliquots. Titrations were performed at ambient temperature with vortexing after each addition of base, using a pH meter, model PHM82 (Radiometer, Copenhagen), with a combination semi-microelectrode (Corning, Corning, NY). Equivalence points were identified at local maxima of first derivative plots (generated by slope determination for each point, using coordinates of the neighboring points). The pH at the midpoint between equivalence points was defined as the $pK_a$ of the drug.

### 2.6. Preparation of RBC

Human blood was obtained from healthy volunteers by venipuncture, and collected in tubes containing citrate anticoagulant. RBC were washed four times by centrifugation, in 150 mM NaCl, and the plasma and buffy coat were discarded. Isolated RBC were resuspended in PBS, and stored at 4 °C until ready for use. Cells were used within 24 h of collection, and all cell samples were stored and incubated in capped plastic tubes. Cells not used within 12 h of collection were incubated briefly at 37 °C in PBS before use, to restore metabolic activity. Such treatment allowed cells used 23 h after venipuncture (with intracellular ATP levels at 45% that found in freshly drawn cells) to restore intracellular ATP levels to 75% of the ATP level in fresh cells (assay conditions described below). Final RBC concentrations were 20% hematocrit (HCT) unless otherwise noted. For incubations lasting 6 h or more, cell suspensions contained antibiotics (80–160 U penicillin/ml, 80–160 μg streptomycin/ml) to inhibit microbial growth.

### 2.7. Generation of graded echinocytic morphologies by slow metabolic depletion

Cell samples were incubated in depletion buffer (glucose-free PBS) for up to 33 h at 37 °C, to deplete intracellular ATP stores. Control samples were incubated concurrently in supplemented buffer (PBS containing 10 mM inosine, 10 mM glucose, and 1 mM adenosine), to keep ATP levels replete. ATP-depleted samples exhibited echinocytic morphology, while control samples retained discocytic morphology, consistent with previous findings [14]. Cells with intermediate degrees of ATP depletion and echinocytosis were generated by (a) removing aliquots of the control sample, (b) washing and resuspending the cells in depletion buffer, and (c) continuing incubation for the times indicated in figure legends. Three to five times during the course of the incubation, all samples were pelleted and resuspended in fresh appropriate buffer. Following incubation, all samples were washed by centrifugation, and treated further as indicated.

### 2.8. Incorporation of exogenous lipid into RBC

Following metabolic depletion, control and depleted samples were treated with 100 μM vanadate for 20–50 min at ambient temperature, to inhibit aminophospholipid translocator activity [15,16]. Control samples then were treated with either DLPC or DLPS SUVs in glucose-free, magnesium-free PBS for 40 min at ambient temperature. Cells were washed by centrifugation and resuspended in glucose-free PBS plus 100 μM vanadate, before further treatment.

### 2.9. Measurement of intracellular ATP (after Ref. [17])

ATP-dependent conversion of the glycolytic intermediate 3-phosphoglycerate was monitored by the coupled oxidation of β-nicotinamide adenine dinucleotide (NADH) to NAD. Cell samples at 20% HCT were diluted 1:1 (v/v) with trichloroacetic acid (TCA, 12% w/v). Following brief centrifugation, supernatants were diluted to 17% (v/v) with a solution containing NADH (0.12 mg/ml) and 3-phosphoglyceric acid (7 mM buffered solution). After addition of glyceraldehyde-3-phosphate dehydrogenase (from rabbit muscle) and 3-phosphoglyceric phosphokinase (from yeast) (final concentrations: 22 and 12 U/ml, respectively), oxidation of NADH was monitored at 340 nm for 12 min at ambient temperature. Concentration

standard deviations for duplicate samples were less than 0.02 mM.

### 2.10. CPZ-induced shape reversal of echinocytes generated by metabolic depletion or exogenous lipid

Following lipid addition in control cells, ATP-depleted and lipid-incorporated RBC samples were allowed to sit at 0 °C for 45 min, before treatment with 150 μM CPZ at 0 °C for 40–65 min. Sample aliquots (less than 1% HCT) were fixed (0.3% glutaraldehyde in glucose-free PBS) before and after CPZ addition, and examined by light microscopy. Individual cells were assigned a score based on shape [18]. Discocytes were assigned a score of 0, while cells exhibiting increasingly perturbed morphology were assigned scores of increasing absolute value: echinocytes were assigned scores from +1 (slightly echinocytic cells) to +5 (spheroechinocytes), and stomatocytes were assigned scores from −1 (monoinvaginated cells) to −4 (spherostomatocytes). The average score of a field of 100 cells was defined as the morphological index (MI) of that sample [19]. Generally, multiple MI determinations of the same sample generated standard deviations between determinations of no more than 0.25 MI units, more typically no more than 0.15 MI units. At these CPZ concentrations, significant drug–membrane interactions are reported, with limited cell lysis [11,12,20–23].

## 3. Results

Unless otherwise indicated, the following results are representative findings from individual experiments.

### 3.1. CPZ fluorescence in model membrane systems

In a study of samples not subjected to ultrafiltration, where only single fluorescence readings were taken per sample, fluorescence of 120 μM CPZ increased with added DLPC to 320% and 370% in the presence of 0.2 and 1.0 mM lipid, respectively (Table 1). A second experiment examined the CPZ fluorescence response to lipid concentrations in the range 0.1–0.5 mM (Fig. 1). Again, dose-dependent fluorescence increases were found as lipid was increased to 0.2 mM, but above that lipid concentration, fluorescence intensity varied little. These results are consistent with formation of a saturable drug–lipid complex. The studies detailed below were carried out using a uniform lipid concentration of 1.0 mM, well into the saturated range of the interaction. This concentration approximates the phospholipid present in a 20% HCT suspension of RBC ([14]; reviewed in Ref. [24]), the HCT employed in whole-cell experiments.

Table 1
Effect of small unilamellar vesicle phospholipid concentration on chlorpromazine fluorescence

| [DLPC], mM | Excitation wavelength, nm | Emission wavelength, nm | CPZ emission signal intensity, cps |
|---|---|---|---|
| 0 | 355 | 457 | $0.54 \times 10^6$ |
| 0.2 | 320 | 456 | $1.72 \times 10^6$ |
| 1.0 | 322 | 451 | $2.02 \times 10^6$ |

CPZ (120 μM) was admixed with sonicated DLPC at the concentrations indicated, then analyzed for CPZ fluorescence emission signal intensity (counts per second, cps) at the indicated wavelengths, selected for maximal emission intensity.

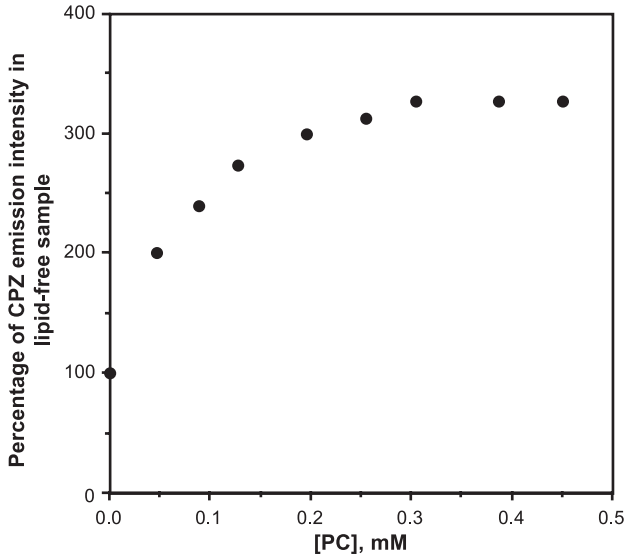


Fig. 1. Effect of phospholipid concentration on fluorescence emission intensity of CPZ. Solutions of CPZ (120 μM in NaCl/Tris buffer) were treated with small unilamellar vesicles composed of sonicated PC (70 mol% DLPC, 30 mol% DMPC) at the total lipid concentrations indicated. Samples then were analyzed for CPZ fluorescence emission signal intensity (wavelength settings: excitation, 325 nm; emission, 453 nm) at ambient temperature without further treatment. Indicated intensity values represent acquisition of single emission readings per sample.

To assess the effect of membrane phospholipid composition on CPZ membrane binding, CPZ (120 μM) was allowed to interact with SUVs containing 0–30 mol% PS, then analyzed for CPZ fluorescence. SUVs without PS were representative of the general lipid environment of the RBC membrane outer leaflet, while SUVs containing 30% PS approximated the lipid environment of the RBC membrane inner leaflet [14]. As PS content was increased from 0% to 30%, the fluorescence of 120 μM CPZ samples increased 92% (Fig. 2, right hand data set). A similar fluorescence enhancement was also observed at lower CPZ concentrations (Fig. 2, center data set).

When incubated with SUV suspensions 0.95 mM in total lipid (Fig. 2), CPZ samples exhibited an increase in emission intensity of 220–250% as drug concentration increased 5-fold (24–120 μM). These dose-dependent increases in CPZ emission intensity with increasing amounts of PS demonstrated the importance of anionic phospholipid (and

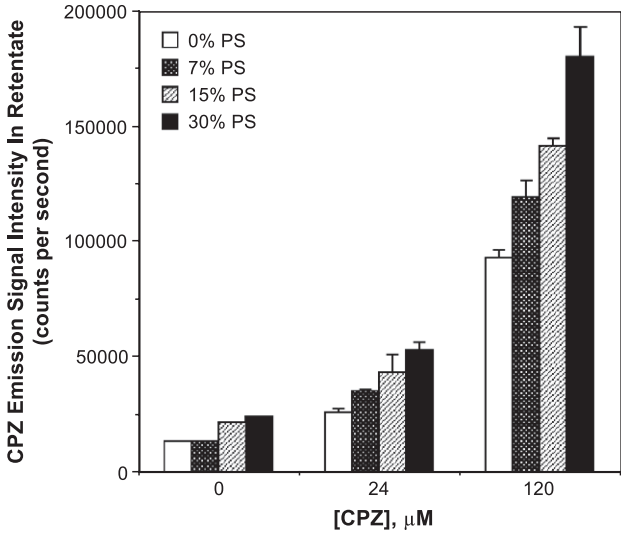


Fig. 2. Effect of PS on fluorescence emission intensity of CPZ at low and high drug concentrations. Solutions of 0 μM CPZ ($n=1$), 24 μM CPZ ($n=2$) or 120 μM CPZ ($n=4$) in NaCl/Tris buffer were incubated with small unilamellar vesicles (0.95 mM sonicated lipid composed of 70 mol% DLPC, DMPS at the mole percentages indicated, with the remaining lipid DMPC) for 45 min at ambient temperature. Each sample was then diluted with one volume NaCl/Tris buffer and subjected to ultrafiltration as described. Retentates were resuspended in NaCl/Tris buffer, diluted 4.4-fold from original sample volumes, and analyzed for fluorescence emission of the fraction of sample CPZ molecules bound to sample SUVs, as described (wavelength settings: excitation, 319 nm; emission, 452 nm). Error bars represent standard deviations.

electrostatic interactions in general) in the binding of CPZ to membrane bilayers.

### 3.2. pH titration of CPZ in model membrane systems

p$K_a$ values of CPZ were determined in model membrane systems for lipid or detergent: CPZ ratios of 8:1–16:1, approximating the ratios of cell lipid/drug used in the cell studies of this and previous investigations [12]. At these ratios and the concentrations indicated, solutions were clear at titration start, with no discernible precipitation and little or no increase in turbidity at higher pH, thereby overcoming such drug effects observed in free aqueous solution [25].

To establish the p$K_a$ of CPZ in a nonionic environment, the drug was titrated in the presence of Triton X-100 micelles. At a concentration of 3.1% (v/v) detergent (detergent/drug molar ratio: 16:1), 3.25 mM CPZ titrated with 0.25 M NaOH produced a curve with equivalence points at pH 5.9 and 9.4, resulting in a calculated p$K_a$ value of 7.8 for this system (Fig. 3A). With Triton X-100 devoid of titratable functionalities in this pH domain, and the nitrogen atom of the CPZ heterocycle expected to titrate at a much lower pH due to resonance stabilization effects, the observed p$K_a$ represented titration exclusively at the propylamine function of CPZ. Because detergent suspensions were in micellar form (reviewed in Ref. [26]) while the following lipid suspensions were in bilayer form, a sample of drug was titrated at a reduced Triton X-100 concentration (detergent/drug molar ratio: 4:1) to correspond to the concentration of bulk lipid molecules exposed to the surrounding aqueous medium in the bilayer samples. The observed p$K_a$ of CPZ was not affected by such reduction in Triton X-100 concentration (data not shown).

To establish the p$K_a$ of CPZ in a zwitterionic phospholipid environment, the drug was titrated in the presence of phospholipid bilayers composed exclusively of phosphatidylcholine (PC). Titration of the propylamine of CPZ (3.25 mM) in the presence of SUVs composed of DLPC and DMPC (22.5 and 2.5 mM, respectively; total lipid/drug molar ratio: 8:1) generated a curve similar in appearance to that with Triton X-100 (Fig. 3B). However, with PC SUVs, the p$K_a$ of the propylamine of CPZ was 8.0, a discernible increase over that with nonionic detergent. The quantity of base needed to traverse from the first equivalence point to the second was comparable when either Triton X-100 or PC was used as the bulk amphiphile, indicating that comparable numbers of CPZ molecules were deprotonated whether the bulk amphiphilic phase was in micellar or bilayer form.

To assess the effect of anionic phospholipid on CPZ titration, DMPS (net charge: $-1$ at pH 7.4) was substituted for DMPC in SUVs and included with CPZ during titration. This system generated only one detectable equivalence point and first derivative maximum (Fig. 3C), producing a simple sigmoidal titration curve. Thus, an accurate determination of CPZ p$K_a$ in the presence of PS was not possible by this methodology. Possibly, concurrent titration of PS may have complicated the titration of the drug [27].

To examine a different anionic lipid, CPZ was titrated in the presence of phosphatidylglycerol (PG). A net anionic lipid having no titratable groups in the pH region of interest ([27], review), PG should not have an independent effect on the titration curve. Titration of 3.25 mM CPZ with SUV suspensions of 22.5 mM DLPC and 2.5 mM DMPG, two well-defined equivalence points were obtained, and the p$K_a$ of CPZ in this system was determined to be 8.3 (Fig. 3D), higher than those in the presence of either Triton X-100 or PC alone. Thus, when excluded from the p$K_a$ range of the drug, the presence of detergent or lipid in suspension with CPZ promoted an increase of CPZ p*K*a with increasing lipid anionicity. These results indicate that association with anionic amphipaths raises the p$K_a$ of CPZ, such that at physiological pH, a larger fraction of the drug is protonated.

### 3.3. Intracellular ATP of echinocytes generated by metabolic depletion or exogenous lipid

Before incubation, initial ATP levels in untreated red cells (at 20% HCT) were determined to be 0.25 mM, consistent with reported values of ATP concentration in normal human red cells [28]. Incubation of cell samples at 37 °C with supplemented PBS for 33 h allowed intracellular ATP levels to double over initial levels (Fig. 4, bars A and B).

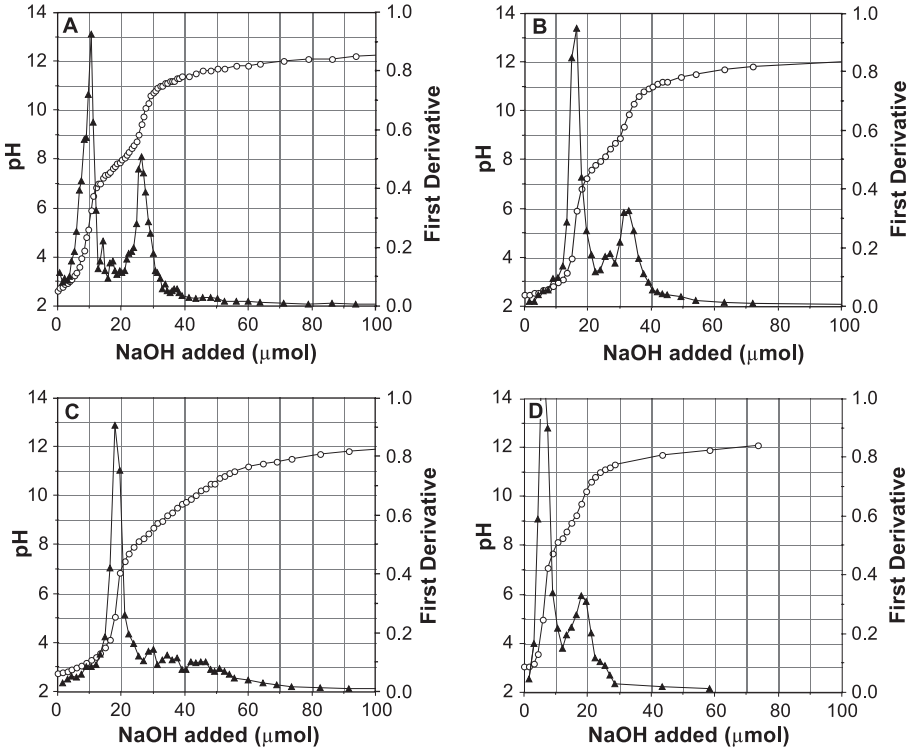


Fig. 3. Titration curve of CPZ in the presence of detergent micelles or phospholipid SUVs. CPZ solutions (3.25 mM) were combined with micelles of 3.1% Triton X-100 (v/v) (A), SUVs of 22.5 mM DLPC plus 2.5 mM DMPC (B), SUVs of 22.5 mM DLPC plus 2.5 mM DMPS (C), or SUVs of 22.5 mM DLPC plus 2.5 mM DMPG (D). Samples then were suspended to an initial volume of 5 ml in 150 mM $NaCl_{(aq)}$. Titration was executed as described to generate the drug titration curve (open circles). Equivalence points were identified at the two peaks of the first derivative plot (filled triangles). The pH at the midpoint between equivalence points was defined as the $pK_a$ of the drug.

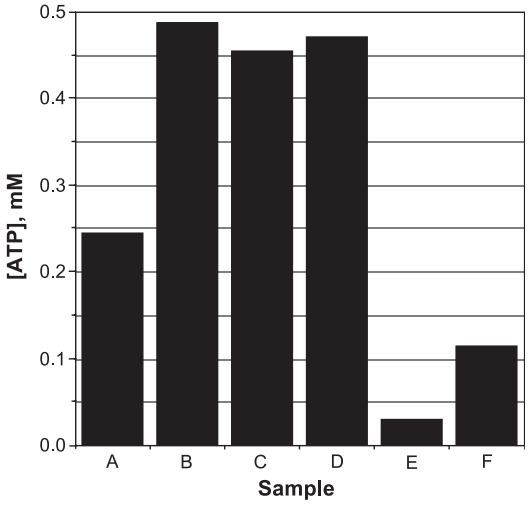


Fig. 4. ATP levels in metabolically depleted and lipid-induced echinocytes (20% HCT). Cell samples were diluted to 20% HCT in the presence (B, C, D) or absence (A, E) of sugar supplementation, then were incubated for 33 h (B, C, D, E) with resuspension of cells twice in fresh buffer during the course of the incubation. Samples in buffer containing 100 μM vanadate then were treated with SUVs for 35 min at ambient temperature. Following removal of unincorporated lipid, samples were diluted 1:1 (v/v) with TCA (12% w/v), then quick-frozen and stored at −20 °C for ATP analysis as described. A: sample before incubation; B, E: no lipid; C: 42 μM DLPS; D: 24 μM DLPC; F: 0.1 mM ATP standard.

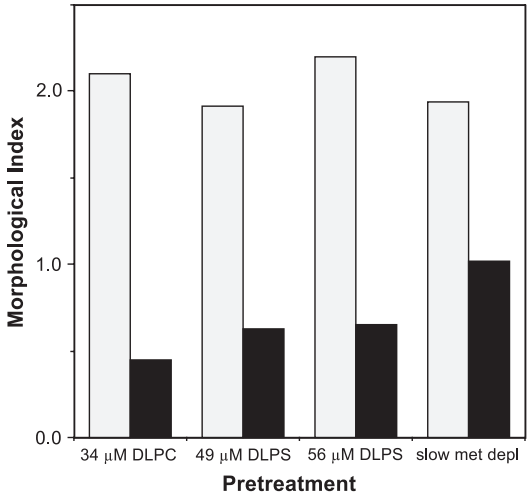


Fig. 5. CPZ-induced shape change of various echinocytes in the presence of vanadate. Cell samples were incubated at 37 °C for up to 31 h with three to four buffer changes in the absence of sugar supplementation to induce metabolic depletion (fourth data set), or in the presence of sugar supplementation to inhibit metabolic depletion. All samples then were washed and pretreated with 100 μM vanadate. Samples subjected to sugar supplementation then were treated with lipid SUVs of DLPC (34 μM) or DLPS (49 or 56 μM) for 40 min at ambient temperature. Samples were washed and morphological indices were determined (gray bars). All samples were then treated with 150 μM CPZ at 0 °C for 20 min, and aliquots were fixed for morphological analysis (filled bars).

Subsequent addition of vanadate followed by DLPS (Fig. 4, bar C) or DLPC (Fig. 4, bar D), producing echinocytic morphology, did not affect this ATP increase significantly. Over the same time period, cells in depletion buffer became echinocytic without the addition of exogenous lipid, while ATP levels in such samples dropped by almost 90% over initial levels (Fig. 4, bar E). Thus, while metabolically depleted echinocytes do not differ in appearance from lipid-incorporated echinocytes, their membranes will be affected by the metabolic depletion process, most notably in reduction in the levels of polyanionic polyphosphoinositide lipids in the inner membrane leaflet [14].

### *3.4. CPZ-induced shape reversal of echinocytes generated by metabolic depletion or exogenous lipid*

The capacity of the stomatogen CPZ to reverse echinocytosis was examined. RBC samples incubated for 31 h in depletion buffer transformed from discocytes (MI = − 0.14) to intermediate-level echinocytes (MI= + 1.94) concurrent with depletion of polyphosphoinositides in the inner bilayer leaflet [14]. Comparable echinocytosis was generated in ATP-replete cells by treatment with exogenous lipid in the presence of vanadate, which inhibits transport of PS to the inner monolayer [15,16]. Control cells were treated with SUVs (DMPC 34 μM; DLPS 49 or 56 μM), producing MIs of approximately + 2 (Fig. 5). These echinocytic samples exhibited different morphological responses to CPZ. The drug reduced the MI of ATP-depleted echinocytes by 50%, while the lipid-induced cells reverted at least 66% (Fig. 5). Shape reversal was blunted slightly in the PS echinocytes over the PC echinocytes, suggesting a slight charge-induced accumulation of the cationic drug in PS-enriched outer leaflets. However, of the samples studied, the least drug-induced shape reversion was found in the metabolically depleted echinocytes. This finding was consistent in experiments starting with varying extents of initial echinocytosis (Fig. 6). Because levels of the phospholipid phosphatidylinositol-4,5-bisphosphate ($PIP_2$) have been shown to diminish during the course of slow metabolic depletion [14], the reduced stomatocytic effect of CPZ in metabolically depleted RBC may be attributed to reduced sequestration of cationic drug molecules in the membrane inner leaflet.

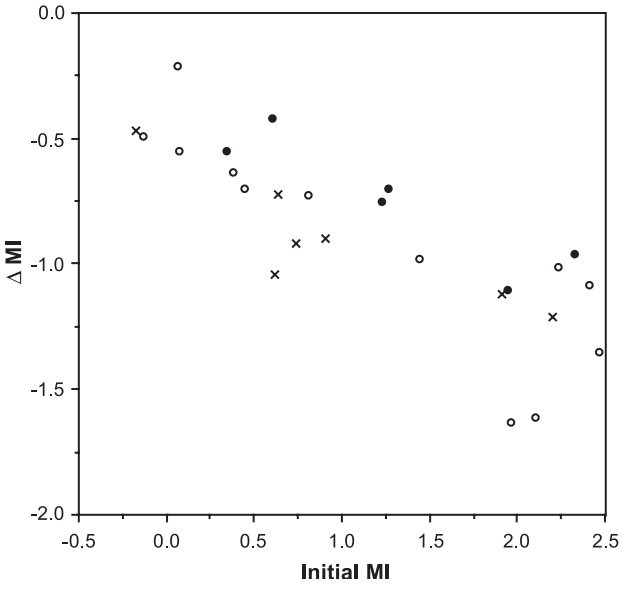


Fig. 6. CPZ-induced shape change of various echinocytes in the presence of vanadate—combined results of several experiments. Cell samples were incubated at 37 °C for up to 33 h with three to five buffer changes in the presence (open circles, × 's) or absence (solid circles) of sugar supplements to induce metabolic depletion. Samples then were washed, pretreated with 100 μM vanadate, and treated with lipid SUVs for 40 min at ambient temperature: no lipid (solid circles), 0–35 μM DLPC (open circles), 30–90 μM DLPS ( × 's). After washing, samples were treated with 150 μM CPZ at 0 °C for 40–65 min, and aliquots were fixed for morphological analysis. *X*-axis, MI before CPZ addition; *Y*-axis, MI after CPZ treatment minus MI before CPZ treatment. Positive ΔMIs indicate echinocytic response to treatment, while negative ΔMIs indicate stomatocytic response. Samples having an initial MI of + 2.5 or greater contained a preponderance of severely echinocytic cells indicative of membrane shedding, and thus were excluded from analysis.

## 4. Discussion

The work of Sheetz and Singer [11] is among the first to assert that CPZ induces stomatocytosis in RBCs by intercalating preferentially into the membrane inner leaflet. Demonstration that net negatively charged phospholipids are localized in the membrane inner leaflet [9,10] provides a physical rationale for the inner leaflet disposition of cationic amphipaths like CPZ [11]. Subsequent studies support the importance of the CPZ charge in membrane binding. Nwafor and Coakley [29] assert that the ionic forms of CPZ and other charged amphipathic drugs participate in Donnan equilibrium across the RBC membrane. When making the membrane potential of RBC samples more positive by reduction of extracellular chloride, they propose that the concentration of CPZ cation associated with the inner leaflet decreases to maintain equilibrium, explaining the observed reduction in stomatocytosis for such samples [29]. Elferink [21] reports spectrophotometric evidence for charge-induced sequestration of CPZ in the inner leaflet, demonstrating that CPZ binds preferentially to the sequestered membrane inner leaflets of both leaky and resealed ghosts. Additionally, Elferink provides spectrophotometric evidence that CPZ binds preferentially to PC liposomes containing (net anionic) PS, compared to PC liposomes, substantiating further the electrostatic component in the binding of cationic amphipaths [21].

However, the above drug binding results are obtained by spectrophotometric determination of unbound drug concentration in the supernatant following centrifugation in the ghost study, and following dialysis in the liposome study [21]. These methods are nonideal in that values must be corrected for ghost lysate contamination and/or nonspecific drug binding to the dialysis membrane [21], also in that drug

binding is determined indirectly through the analysis of unbound drug levels, which often are too low to detect with consistent accuracy. Recent studies employing NMR, calorimetric, and Langmuir techniques also emphasize the importance of electrostatic interactions in CPZ membrane lipid binding, though possible effects of sample pH, phospholipid acyl chain length, and membrane rigidity on their findings warrant further investigation [30,31].

The present investigation expands upon these previous studies by providing direct controlled evidence of an electrostatic interaction between CPZ and anionic components of the membrane inner leaflet. CPZ fluorescence provides one such direct measurement of drug binding to model membranes. According to fluorescence theory, increased CPZ fluorescence indicates an increase in drug binding to a second component, such as a model membrane system; this binding should restrict drug vibrational movement, resulting in greater energy dissipation through increased fluorescence emission intensity [32]. Moreover, because CPZ is a highly lipophilic molecule, with a reported partition coefficient into PC vesicles of about 3500 at 100 μM drug and 1 mg $ml^{-1}$ lipid [13], the sample fraction of CPZ bound to model membranes typically is at quantities large enough to detect accurately and consistently.

The drug fluorescence studies indicate that the hydrophobic nature of CPZ drives its general association with membranes, while the cationic nature of CPZ promotes its preferential association with the membrane inner leaflet. Fluorescence of 120 μM CPZ increases when sonicated zwitterionic lipid (PC) is present, by 320–370% when at least 0.2 mM in lipid. Drug fluorescence is enhanced further (up to 92% over PC alone) when the lipid composition is up to 30 mol% PS. This approximates the percentage of PS found in the membrane inner leaflet of RBC [14].

The p$K_a$ of CPZ also provides a direct measurement of drug–membrane binding. Insertion into a hydrophobic environment would be expected to stabilize the deprotonated molecule, lowering the observed p$K_a$. Conversely, if the cationic nature of CPZ contributes significantly to binding with anionic membrane components, a higher pH will be required to deprotonate the drug when in an anionic environment than when in a neutral or zwitterionic environment. As a result, the p$K_a$ of CPZ should increase as the anionic nature of the membrane increases.

Results of the drug p$K_a$ studies verify the presence of dominant hydrophobic and significant ancillary electrostatic interactions in CPZ membrane binding. Hydrophobic interaction is evident particularly when assessing the p$K_a$ of CPZ in the presence of Triton X-100, a nonionic polyethylene glycol ether. In 3.1% (v/v) Triton X-100, a detergent concentration well above the critical micelle concentration (reviewed in Ref. [26]), CPZ (3.25 mM) exhibits a p$K_a$ of 7.8, significantly lower than the reported p$K_a$ values of 8.6–9.2 for CPZ in free aqueous solution [25,33].

In agreement with the fluorescence studies, results of the p$K_a$ studies indicate an increase in drug–membrane binding as amphipath negative charge density increases, from nonionic (Triton X-100) to zwitterionic (PC) to anionic (PC with PG). In the presence of PC SUVs (25 mM lipid), pH titration of CPZ (3.25 mM) discloses a drug p$K_a$ value of 8.0, a small but discernible increase from the value observed with Triton X-100. This p$K_a$ value is attributable to the drug, because the phospholipid functional groups titrate well away from the observed p$K_a$ range [27]. Moreover, this increase in drug p$K_a$ is unaffected when Triton X-100 concentration in the micellar sample is reduced 4-fold to match the lipid concentration in the membrane outer leaflet of the PC sample. Thus, while PC is net neutral at physiological pH, the presence of charge on the lipid enhances drug binding over that observed with nonionic detergent.

Incorporation of net anionic phospholipid into SUVs should increase the p$K_a$ of CPZ even further, indicating additional enhancement of drug–membrane binding over that observed with nonionic and zwitterionic amphipathic phases. Making the lipid 10% in the anionic phospholipid PS results in a titration curve with no discernible p$K_a$ value (Fig. 3C), due possibly to concurrent titration of CPZ and the terminal PS amine group [27]. Substitution of PG for PS produces a drug p$K_a$ value of 8.3 (Fig. 3D), indicating the strongest drug/lipid interaction of any of the systems studied. These titration studies demonstrate a preferential interaction between CPZ and anionic membrane lipid components.

Collectively, these fluorescence and p$K_a$ studies support a mechanism by which CPZ accumulates spontaneously in the cell membrane inner leaflet by a combination of hydrophobic and electrostatic interactions. At the outer membrane surface, composed mainly of zwitterionic lipid, the p$K_a$ of CPZ is around 8.0. At pH 7.4, approximately 25% of the CPZ population should be electroneutral and capable of partitioning into the hydrophobic phase [11,21]. As mass action generates more unprotonated drug, most CPZ at the outer surface can be incorporated into the bilayer. Once in the bilayer, the propylamine function eventually encounters the anionic headgroups of the membrane inner leaflet. Exposed to the cytoplasmic surface and the cytoplasm at physiological pH, the terminal amine group reprotonates and binds with the anionic phospholipids present in the inner leaflet. In this manner, drug molecules accumulate preferentially in the membrane inner leaflet, resulting in stomatogenic inner leaflet expansion.

It has been shown that the MI scale (and the cell shape progressions represented therein) is continuous, and that morphologies can be reversed by inducing expansion of the opposing membrane leaflet [34,35]. Thus, it is possible to use CPZ to revert echinocytic cells to more discocytic morphologies (Fig. 5). The present study takes advantage of this CPZ-induced shape reversion to develop a methodology for in situ assessment of drug interactions with specific anionic lipid components.

To test if CPZ membrane binding is driven by specific association with membrane PS, CPZ-induced shape reversal

was examined in echinocytes generated by exposure to exogenous PC or PS, in the presence of vanadate. This treatment inhibits the aminophospholipid translocator, trapping exogenous PS as well as PC in the outer leaflet [15,16]. Should CPZ bind preferentially to PS, then the drug should partition more evenly between the two membrane leaflets in PS-induced echinocytes, resulting in less extensive reversal of echinocytosis compared to PC-treated samples. This difference is observed, but the extent is minor (Figs. 5 and 6). It is likely that the amount of exogenous PS loaded into the outer leaflet is small relative to the endogenous PS in the inner leaflet [14,36], so the effect would be expected to be subtle.

To assess the importance of phosphatidic acid (PA), phosphatidylinositol (PI), and the polyphosphoinositides in CPZ–membrane binding, CPZ-induced shape reversal was compared for echinocytes produced by slow metabolic depletion and cells made echinocytic by exogenous PC or PS. The process of slow metabolic depletion (Fig. 4) results in net dephosphorylation of PA to diacylglycerol (DAG) and of $PIP_2$ to PI [14]. Thus, treatment is similar to PS echinocytosis in reducing the ratio of inner leaflet/outer leaflet negative charge, while affecting the transbilayer distribution of PS very little [37].

Echinocytes generated by slow metabolic depletion and then treated with CPZ exhibit much less shape reversal than echinocytes generated by exogenous lipid (Figs. 5 and 6). Because these CPZ incubations were performed at 0 °C, the observed diminished shape change reversal cannot be attributed to the drug-induced movement of endogenous PS to the membrane outer leaflet, which is observed at higher incubation temperatures [12,38]. The observed reduction in shape change reversal also does not appear to be due to reduced cell deformability. Metabolic depletion has been reported to decrease cell deformability [39], which could explain the inhibition of drug-induced shape change in such samples. A more recent report indicates that echinocytes generated by metabolic depletion exhibit the same decreased deformability as replete echinocytes generated by salicylic acid [40].

The shape reversal results implicate PA and $PIP_2$ as probable binding sites for CPZ. PS is the major negatively charged lipid in the inner monolayer, making up roughly 30 mol% of inner monolayer phospholipid and 60% of lipid negative charge [10,14,41–43]. However, PA, PI and the polyphosphoinositides, while collectively composing only 9 mol% of phospholipid, contribute 40% of the net anionic charge [10,14,41–43]. Thus, a small change in the molar levels of these latter lipids can result in significant changes to inner leaflet anionicity, and possibly to the inner leaflet propensity of CPZ.

As reported earlier [14], both PA dephosphorylation to DAG, and $PIP_2$ net dephosphorylation to PI contribute equally to the combined membrane inner leaflet shrinkage and outer leaflet expansion leading to echinocytosis in metabolic depletion. Using values of headgroup surface areas calculated by J.E. Ferrell (personal communication), dephosphorylation of one PA molecule to DAG results in membrane inner leaflet shrinkage of 11 $Å^2$. Assuming that DAG distributes evenly between inner and outer leaflet [44], the inner leaflet shrinks by an additional 13 $Å^2$, while the outer leaflet expands by the same amount. Thus, the net relative outward expansion from the dephosphorylation of one molecule of PA is 37 $Å^2$. Per molecule of $PIP_2$ dephosphorylated to PI, the inner leaflet surface area contracts by 25 $Å^2$ [14]. Because similar shrinkage is attributable to the net conversion of $PIP_2$ to PI as with the conversion from PA to DAG [14], a shrinkage of 37 $Å^2$ results from roughly 1.5 molecules of $PIP_2$. From these calculations, degradation of 1 molecule of PA plus 1.5 molecules of $PIP_2$ reduces the number of inner monolayer negative charges by about 7 [i.e., $1+(1.5\times4)$], for a net inner leaflet shrinkage of roughly 74 $Å^2$. In contrast, a similar expansion (74 $Å^2$) in outer leaflet surface area resulting from intercalation of exogenous PS, resulting from insertion of 1 to 2 PS molecules, would generate a net negative charge gain of only 1–2. Thus, for the same level of echinocytosis, the net shift in negative charge toward the outer leaflet is about 3.5 to 7 times greater for metabolically depleted echinocytes than for PS-loaded echinocytes. These calculations indicate that the amount of exogenous PS loaded into PS echinocytes is not sufficient to allow direct comparisons with the metabolically depleted echinocytes. These findings alone neither confirm nor exclude selective CPZ binding to PS.[3]

However, closer analysis of the physical quantities of lipid and drug in the RBC membrane lends support to the assertion that CPZ molecules bind to polyphosphoinositide lipid molecules in preference to PS. The polyphosphoinositides provide 340 μmol of net monovalent negative charge per liter of RBC (calculated from values in Ref. [14]). Assuming total membrane incorporation of CPZ, a sample of 120 μM CPZ in a 20% HCT suspension of cells yields a final intramembrane CPZ concentration of 600 μmol/l of RBC. Thus, the polyphosphoinositides provide enough monovalent sites for roughly half the drug molecules. The remaining drug may be retained in the membrane hydrocarbon phase as neutral species [22], or bound by other anionic phospholipids, with PS providing 570 μmol of net negative charge per liter of cells (calculated from values in Ref. [14]). Indeed, if CPZ has no preference for a specific anionic phospholipid headgroup, then the inner leaflet population of PS alone should provide enough binding sites for most all the incorporated drug molecules. This situation arises in metabolic depletion, where polyphosphoinositide levels are reduced [14] while PS levels in the inner leaflet tend not to fluctuate greatly [37]. (This analysis excludes the likely

[3] Calculated values presented in the Discussion section herein are based on total inner leaflet localization of native anionic phospholipid in normal RBC membranes, though reports indicate that 20 mol% of membrane PA, PI, and $PIP_2$ reside in the outer leaflet [42,43]. The resulting conclusions are qualitatively unaffected by this difference.

binding of CPZ to cytosolic proteins, which would afford additional anchorage sites.)

However, CPZ-induced shape reversion is inhibited significantly in metabolically depleted cells, indicating that cationic CPZ molecules do not associate as readily with PS as with polyphosphoinositide lipid molecules. The higher negative charge density of the polyphosphoinositides may offer more stable binding sites for the charged CPZ.

The above data and calculations indicate that polyphosphoinositide lipids provide the preponderance of CPZ binding sites in the membrane inner leaflet, a conclusion consistent with previous findings. For instance, it is shown that incubation of RBC with CPZ up to 2 days at 37 °C results in elevated polyphosphoinositide levels compared to CPZ-free control samples [45]. Such an effect possibly is due to physical drug–lipid association, making the lipids sterically inaccessible to dephosphorylation by phosphatases. The connection between CPZ and the polyphosphoinositides also is evident at the neuronal level: CPZ blocks $\alpha_1$-adrenergic receptors ([1], review), whose activation ordinarily would result in up-regulation of $PIP_2$ phosphodiesterases as an intermediary step in neuronal activation [3]. Thus, the possibility that CPZ could inhibit enzymatic $PIP_2$ degradation by direct physical interaction with these lipids in the membrane would provide an alternative pathway by which neuroleptic effects could be elicited.

Other studies indicate that CPZ also interacts with protein components in the membrane, [46], such as spectrin [47,48]. Spectrin has sites of phosphorylation regulated by calmodulin-dependent spectrin kinases [49], and the possibility of CPZ binding to membrane proteins (perhaps at phosphorylation sites) is not excluded by the current investigation. Ongoing studies will ascertain the relative contributions of membrane protein and lipid binding to the observed CPZ-induced shape effects.

## Acknowledgements

The authors thank Nicole Leonard and Carla Morada for technical assistance. J.Y.C. also thanks the faculty of Stanford's Chemistry and Radiology departments for helpful discussion.

## References

[1] S.C. Dilsaver, Antipsychotic agents: a review, Am. Fam. Phys. 47 (1993) 199–204.
[2] E. Richelson, Neuroleptics and neurotransmitter receptors, Psychiatr. Ann. 10 (1980) 21–40.
[3] R.J. Baldessarini, Chemotherapy in Psychiatry: Principles and Practice, Harvard Univ. Press, Cambridge, MA, 1985.
[4] R.J. Baldessarini, Drugs and the treatment of psychiatric disorders, in: A.G. Gilman, L.S. Goodman, T.W. Rall, F. Murad (Eds.), The Pharmacological Basis of Therapeutics, 7th ed., Macmillan Publishing, New York, 1985, pp. 387–445.
[5] J.M. Kane, Schizophrenia, N. Engl. J. Med. 334 (1996) 34–41.
[6] J.R. Bianchine, Drugs for Parkinson's disease, spasticity, and acute muscle spasms, in: A.G. Gilman, L.S. Goodman, T.W. Rall, F. Murad (Eds.), The Pharmacological Basis of Therapeutics, 7th ed., Macmillan Publishing, New York, 1985, pp. 473–490.
[7] C. Korth, B.C.H. May, F.E. Cohen, S.B. Prusiner, Acridine and phenothiazine derivatives as pharmacotherapeutics for prion disease, Proc. Natl. Acad. Sci. U. S. A. 98 (2001) 9836–9841.
[8] Y. Kuroda, K. Kitamura, Intra- and intermolecular $^1H-^1H$ nuclear Overhauser effect studies on the interactions of chlorpromazine with lecithin vesicles, J. Am. Chem. Soc. 106 (1984) 1–6.
[9] M.S. Bretscher, Asymmetrical lipid bilayer structure for biological membranes, Nat. New Biol. 236 (1972) 11–12.
[10] A.J. Verkleij, R.F.A. Zwaal, B. Roelofsen, P. Comfurius, D. Kastelijn, L.L.M. Van Deenen, The asymmetric distribution of phospholipids in the human red cell membrane: a combined study using phospholipases and freeze-etch electron microscopy, Biochim. Biophys. Acta 323 (1973) 178–193.
[11] M.P. Sheetz, S.J. Singer, Biological membranes as bilayer couples. A molecular mechanism of drug–erythrocyte interactions, Proc. Natl. Acad. Sci. U. S. A. 71 (1974) 4457–4461.
[12] J.Y. Chen, W.H. Huestis, Role of membrane lipid distribution in chlorpromazine-induced shape change of human erythrocytes, Biochim. Biophys. Acta 1323 (1997) 299–309.
[13] M. Luxnat, H. Galla, Partition of chlorpromazine into lipid bilayer membranes: the effect of membrane structure and composition, Biochim. Biophys. Acta 856 (1986) 274–282.
[14] J.E. Ferrell, W.H. Huestis, Phosphoinositide metabolism and the morphology of human erythrocytes, J. Cell Biol. 98 (1984) 1992–1998.
[15] D.L. Daleke, Maintenance of Cell Membrane Aminophospholipid Asymmetry, PhD Thesis, Stanford University, 1986.
[16] M. Bitbol, P. Fellmann, A. Zachowski, P.F. Devaux, Ion regulation of phosphatidylserine and phosphatidylethanolamine outside–inside translocation in human erythrocytes, Biochim. Biophys. Acta 904 (1987) 268–282.
[17] H. Adam, Adenosine-5′-triphosphate: determination with phosphoglycerate kinase, in: H. Bergmeyer (Ed.), Methods of Enzymatic Analysis, Academic Press, New York, 1963, pp. 539–543.
[18] M. Bessis, Red cell shapes. An illustrated classification and its rationale, in: M. Bessis, R.I. Weed, P.F. Leblond (Eds.), Red Cell Shape: Physiology, Pathology, Ultrastructure, Springer Verlag, New York, 1973, pp. 1–25.
[19] T. Fujii, T. Sato, A. Tamura, M. Wakatsuki, Y. Kanaho, Shape changes of human erythrocytes induced by various amphipathic drugs acting on the membrane of the intact cells, Biochem. Pharmacol. 28 (1979) 613–620.
[20] J. Rosso, A. Zachowski, P.F. Devaux, Influence of chlorpromazine on the transverse mobility of phospholipids in the human erythrocyte membrane: relation to shape changes, Biochim. Biophys. Acta 942 (1988) 271–279.
[21] J.G.R. Elferink, The asymmetric distribution of chlorpromazine and its quaternary analogue over the erythrocyte membrane, Biochem. Pharmacol. 26 (1977) 2411–2416.
[22] M.R. Lieber, Y. Lange, R.S. Weinstein, T.L. Steck, Interaction of chlorpromazine with the human erythrocyte membrane, J. Biol. Chem. 259 (1984) 9225–9234.
[23] J.L. Olivier, C. Chachaty, C. Wolf, D. Daveloose, G. Bereziat, Binding of two spin-labelled derivatives of chlorpromazine to human erythrocytes, Biochem. J. 264 (1989) 633–641.
[24] M.M. Wintrobe, G.R. Lee, D.R. Boggs, T.C. Bithell, J. Foerster, J.W. Athens, J. Lukens, The mature erythrocyte, Clinical Hematology, 8th ed., Lea and Febiger, Philadelphia, 1981, pp. 75–107.
[25] E. Wajnberg, M. Tabak, P.A. Nussenzveig, C.M.B. Lopes, S.R.W. Louro, pH-dependent phase transition of chlorpromazine micellar solutions in the physiological range, Biochim. Biophys. Acta 944 (1988) 185–190.
[26] R.B. Gennis, Biomembranes: Molecular Structure and Function, Springer-Verlag, New York, 1989.

[27] J. Tocanne, J. Teissié, Ionization of phospholipids and phospholipid-supported interfacial lateral diffusion of protons in membrane model systems, Biochim. Biophys. Acta 1031 (1990) 111–142.
[28] E. Beutler, Red Cell Metabolism: A Manual of Biochemical Methods, 3rd ed., Grune and Stratton, Orlando, 1984.
[29] A. Nwafor, W.T. Coakley, Drug-induced shape change in erythrocytes correlates with membrane potential change and is independent of glycocalyx charge, Biochem. Pharmacol. 34 (1985) 3329–3336.
[30] W. Nerdal, S.A. Gundersen, V. Thorsen, H. Hoiland, H. Holmsen, Chlorpromazine interaction with glycerophospholipid liposomes studied by magic angle spinning solid state $^{13}$C-NMR and differential scanning calorimetry, Biochim. Biophys. Acta 1464 (2000) 165–175.
[31] A.V. Agasosler, L.M. Tungodden, D. Cejka, E. Bakstad, L.K. Sydnes, H. Holmsen, Chorpromazine-induced increase in dipalmitoylphosphatidylserine surface area in monolayers at room temperature, Biochem. Pharmacol. 61 (2001) 817–825.
[32] D.A. Skoog, F.J. Holler, T.A. Nieman, Principles of Instrumental Analysis, 5th ed., Harcourt Brace, Philadelphia, 1998.
[33] L.G. Chatten, L.E. Harris, Relationship between p$K_b$($H_2O$) of organic compounds and $E_{1/2}$ values in several nonaqueous solvents, Anal. Chem. 34 (1962) 1495–1501.
[34] D.L. Daleke, W.H. Huestis, Erythrocyte morphology reflects the transbilayer distribution of incorporated phospholipids, J. Cell Biol. 108 (1989) 1375–1385.
[35] D.L. Daleke, W.H. Huestis, Incorporation and translocation of aminophospholipids in human erythrocytes, Biochemistry 24 (1985) 5406–5416.
[36] J.E. Ferrell, K. Lee, W.H. Huestis, Membrane bilayer balance and erythrocyte shape: a quantitative assessment, Biochemistry 24 (1985) 2849–2857.
[37] M.S. Moxness, Effect of Hemoglobin Oxidation on Phospholipid Organization in the Human Erythrocyte, PhD Thesis, Stanford University, 1994.
[38] S.L. Schrier, A. Zachowski, P.F. Devaux, Mechanisms of amphipath-induced stomatocytosis in human erythrocytes, Blood 79 (1992) 782–786.
[39] R.I. Weed, P.L. LaCelle, E.W. Merrill, G. Craib, A. Gregory, F. Karch, F. Pickens, Metabolic dependence of red cell deformability, J. Clin. Invest. 48 (1969) 795–809.
[40] A. Chabanel, W. Reinhart, S. Chien, Increased resistance to membrane deformation of shape-transformed human red blood cells, Blood 69 (1987) 739–743.
[41] A. Brovelli, Erythrocyte membrane damage in hemolytic anemias, Blood Cell Biochem. 1 (1990) 455–474.
[42] P. Bütikofer, Z.W. Lin, D.T. Chiu, B. Lubin, F.A. Kuypers, Transbilayer distribution and mobility of phosphatidylinositol in human red blood cells, J. Biol. Chem. 265 (1990) 16035–16038.
[43] P. Gascard, D. Tran, M. Sauvage, J.C. Sulpice, K. Fukami, T. Takenawa, M. Claret, F. Giraud, Asymmetric distribution of phosphoinositides and phosphatidic acid in the human erythrocyte membrane, Biochim. Biophys. Acta 1069 (1991) 27–36.
[44] D. Allan, P. Thomas, R.H. Michell, Rapid transbilayer diffusion of 1,2-diacylglycerol and its relevance to control of membrane curvature, Nature 276 (1978) 289–290.
[45] P. Bütikofer, Z.W. Lin, F.A. Kuypers, M.D. Scott, C. Xu, G.M. Wagner, D.T. Chiu, B. Lubin, Chlorpromazine inhibits vesiculation, alters phosphoinositide turnover and changes deformability of ATP-depleted RBCs, Blood 73 (1989) 1699–1704.
[46] J.G.R. Elferink, Fluorescence studies of membrane interactions of chlorpromazine and chlorimipramine, Biochem. Pharmacol. 26 (1977) 511–515.
[47] M. Minetti, A.M.M. Di Stasi, Involvement of erythrocyte skeletal proteins in the modulation of membrane fluidity by phenothiazines, Biochemistry 26 (1987) 8133–8137.
[48] A. Enomoto, Y. Takakuwa, S. Manno, A. Tanaka, N. Mohandas, Regulation of erythrocyte ghost membrane mechanical stability by chlorpromazine, Biochim. Biophys. Acta 1512 (2001) 285–290.
[49] M.J. Nelson, D.L. Daleke, W.H. Huestis, Calmodulin-dependent spectrin kinase activity in resealed human erythrocyte ghosts, Biochim. Biophys. Acta 686 (1982) 182–188.